Immunocyte count combined with CT features for distinguishing pulmonary tuberculoma from malignancy among non-calcified solitary pulmonary solid nodules

Zihao Liu, Haoyu Ran, Xiran Yu, Qingchen Wu, Cheng Zhang

Department of Cardiothoracic Surgery, The First Affiliated Hospital of Chongqing Medical University, Chongqing, China
Contributions: (I) Conception and design: Q Wu, C Zhang, Z Liu; (II) Administrative support: Q Wu; (III) Provision of study materials or patients: Z Liu, H Ran, X Yu; (IV) Collection and assembly of data: Z Liu, H Ran, X Yu; (V) Data analysis and interpretation: Z Liu; (VI) Manuscript writing: All authors; (VII) Final approval of manuscript: All authors.
Correspondence to: Qingchen Wu, PhD, MD; Cheng Zhang, PhD, MD. Department of Cardiothoracic Surgery, The First Affiliated Hospital of Chongqing Medical University, Chongqing 400016, China. Email: wuqc6@hotmail.com; zhangcs05223@163.com.

Background: Tuberculoma is the most common type of surgically removed benign solid solitary pulmonary nodule (SPN) and can lead to a high risk of misdiagnoses for clinicians. This study aimed to discuss the value of the immunocyte count combined with computed tomography (CT) features in distinguishing pulmonary tuberculoma from malignancy among non-calcified solid SPNs.

Methods: Forty-eight patients with pulmonary tuberculoma and 52 patients with lung cancer were retrospectively included in our study. Univariate and multivariate analyses were conducted to screen the independent predictors. Receiver operating characteristic (ROC) analysis was performed to investigate the validity of the predictive model.

Results: The univariate and multivariate analyses revealed that a coarse margin, vacuole, lobulation, pleural indentation, cluster of differentiation (CD)3^{+} T-lymphocyte count, and CD4^{+} T-lymphocyte count were independent predictors for distinguishing pulmonary tuberculoma from malignancy. The sensitivity, specificity, accuracy, and the area under the ROC curve of the model comprising the CD3^{+} T-lymphocyte count were 79.2%, 75%, 74.5%, and 0.845 [95% confidence interval (CI), 0.759–0.910], respectively, and those of the model involving the CD4^{+} T-lymphocyte count were 77.1%, 78.8%, 77.1%, and 0.857 (95% CI, 0.773–0.919), respectively.

Conclusions: Immunocyte count combined with CT features is efficient in distinguishing pulmonary tuberculoma from malignancy among non-calcified solid SPNs and has applicable clinical value.

Keywords: Solitary pulmonary nodule (SPN); non-calcified tuberculoma; computed tomography features; immunocyte count

Introduction

Tuberculosis (TB) has again become the most threatening infectious disease in the world, and the burden of TB in China remains substantial (1,2). Tuberculoma is a spherical caseous necrotic lesion wrapped in fibrous tissue that is usually secondary to TB infection. Pulmonary tuberculoma is seen in about 9% of primary TB patients (3). However, many patients with pulmonary tuberculoma have no clear previous TB history and are only examined by physical examination.

On computed tomography (CT) imaging, pulmonary tuberculoma often appears as a solitary pulmonary nodule (SPN), which refers to a single, focal, and circular opacity <3 cm in diameter that is surrounded by pulmonary

parenchyma without other abnormal signs, such as atelectasis, enlarged lymph nodes, or pleural effusion (4). SPNs can be divided into two groups: solid and subsolid (5). Various studies (6,7) have shown that solid SPNs are extremely common, with a considerable portion of these being malignant. The identification of benign and malignant solid SPNs has been a significant challenge for clinicians. For such a small lesion with variable features, clinicians aim to strike a balance between conservative follow-up and direct medical intervention.

Tuberculoma is the most common type of benign SPN, accounting for approximately 25% of all surgically removed SPNs, and often manifests as a solid SPN (8). The treatment of pulmonary tuberculoma is dominated by chemotherapy and is treated by surgery only if the pulmonary tuberculoma does not respond to chemotherapy. However, this lack of a response is indistinguishable from malignancy and leads to extensive destruction (9). Therefore, if pulmonary tuberculoma can be identified by non-surgical approaches, some patients can avoid surgical biopsy. This will not only protect their lung function as much as possible but their financial burden can also be alleviated.

Currently, CT imaging data can assist in distinguishing pulmonary TB from lung cancer among solid SPNs. Typical pulmonary tuberculomas are round, well-defined lesions surrounded by satellite lesions, and calcification can be found in 20–30% of them (10). However, in clinical practice, they can sometimes appear as non-calcified solid SPNs with atypical imaging characteristics such as a coarse margin, vacuole, lobulation, spiculation, and pleural indentation. In enhanced scanning, tuberculomas at different inflammatory stages will exhibit different enhanced characteristics that are similar to lung cancers, thus increasing the risk of misdiagnoses for clinicians (10,11).

Although the SPN detection rate has increased considerably with the appearance of finer CT imaging sections and higher resolution images, the subjectivity of clinicians also leads to many false-positive results (12). In addition, various studies (13,14) have shown that some unique indicators on positron emission tomography (PET)/ CT images, such as maximum uptake values (SUVmax), metabolic tumor volume (MTV), total lesion glycolysis (TLG), and density, are specific for differentiating between pulmonary tuberculoma and lung malignancy and can assess whether the pulmonary tuberculoma is active. However, PET/CT has a high cost and has low sensitivity, specificity, and accuracy for diagnosing small or heterogeneous lesions due to the existence of a partial volume effect (15).

Recently, studies have demonstrated that radiomics nomogram models have some diagnostic efficacy for the differentiation of solid SPNs but their reproducibility and stability require further study and validation (16,17). Tumor-related markers, such as cytokeratin fragment antigen 21-1 (CYFRA21-1), carcinoembryonic antigen (CEA), and others, have been investigated for lung cancer screening in several clinical trials; however, they seemed to exhibit no significant diagnostic efficacy for early lung cancer (18). Thus, distinguishing pulmonary tuberculoma from malignancy among non-calcified solid SPNs remains an urgent problem.

There are three formation mechanisms of tuberculoma: (I) the caseous necrosis is wrapped up in fibrous tissue hyperplasia when the infiltrative pulmonary TB is cured; (II) the TB cavity is concentrated because the bronchus connected with it is obstructed; and (III) the primary pulmonary TB appears as a circular lesion (19). Nevertheless, regardless of how it is formed, a tuberculoma is considered to have the characteristic caseous granuloma. $CD3^+$ T cells and their subsets (such as $CD4^+$ T cells, $CD8^+$ T cells, and other immune cells) play an important role in the formation of tuberculous granuloma and the development of pulmonary TB (20-23). Recent articles (24,25) have shown that their downstream cytokines, such as interleukin (IL), tumor necrosis factor-α (TNF-α), and interferon-γ (IFN-γ), are valuable for the identification of SPNs. At the same time, the development of malignant

---

Highlight box

Key findings

• The immunocyte count may be used as a potential indicator for distinguishing pulmonary tuberculoma from early malignancy, which will be a starting point for further research.

What is known and what is new?

• Currently, computed tomography (CT) imaging data can assist in distinguishing pulmonary tuberculosis (TB) from lung cancer among solid solitary pulmonary nodules (SPNs). The immunocyte count combined with CT features can enhance the diagnostic power.

What is the implication, and what should change now?

• Our study demonstrated that clinicians need to be highly vigilant for pulmonary tuberculoma in cases of non-calcified solid SPNs without a coarse margin, vacuole, lobation, spiculation, and pleural indentation combined with high cluster of differentiation $(CD)3^+$ or $CD4^+$ T-cell counts. Follow-up is recommended for these patients.

tumors requires the body to be in a low immune reaction state (26).

Therefore, we propose to evaluate the clinical, immunologic, and imaging features to screen out the critical characteristics for distinguishing pulmonary tuberculoma from lung cancer among non-calcified solid SPNs and to build an accurate and clinically practical diagnostic model. We present the following article in accordance with the STROBE reporting checklist (available at https://jtd. amegroups.com/article/view/10.21037/jtd-22-1024/rc).

Methods

Patients

Patients with indeterminate solid SPNs who visited the First Affiliated Hospital of Chongqing Medical University from January 2018 to June 2022 and were diagnosed by surgical biopsies were retrospectively collected. The inclusion criteria were as follows: patients who were surgically diagnosed with pulmonary tuberculoma or malignancy and had definite postoperative pathological results. The exclusion criteria were as follows: (I) patients with pulmonary nodules that did not appear as non-calcified solid SPNs; (II) patients who had recently received anti-infection therapy, anti-TB therapy, or anti-tumor chemotherapy; (III) patients that were previously diagnosed with lung cancer; (IV) patients who were taking drugs that have an impact on immune function, such as glucocorticosteroids, immunoglobulins, and interferons; (V) patients with acute pneumonia or infections in other parts of the body; (VI) patients with autoimmune diseases or other immune system diseases; (VII) patients with severe cardiac, hepatic, or renal abnormalities; and (VIII) patients with a history of malignancies in other systems. The study was conducted in accordance with the Declaration of Helsinki (as revised in 2013). The study was approved by Clinical Research Ethics Committee of the First Affiliated Hospital of Chongqing Medical University (No. 2022-375) and informed consent was obtained from all subjects.

Two clinicians conducted a review of the patients' clinical data obtained from the electronic medical records, including gender, age, history of TB, history of heavy smoking, CYFRA21-1, CEA, as well as indicators related to the body's immune function in peripheral blood, such as lymphocyte count, CD3$^+$ T-cell count, CD4$^+$ T-cell count, CD8$^+$ T-cell count, and the ratio of CD4$^+$ T-lymphocyte count to CD8$^+$ T-lymphocyte count (CD4$^+$ T/CD8$^+$ T).

CT image acquisition and description

Chest CT scans were conducted using the SOMATOM Perspective (Siemens Healthineers, Erlangen, Germany), and SOMATOM Definition Flash (Siemens Healthineers, Erlangen, Germany) CT scanner according to the following protocol parameters: patients were in a supine position, and the range was from the apex to the costophrenic angle. Additional parameters were as follows: 90–130 KVp; 50–140 mAs; rotation speed, 0.5 r/s; pitch, 1; slice thickness and interval for axial images, 5 mm/5 mm; and reconstruction by standard algorithm or medium-sharp algorithm after scanning, 1 mm/1 mm.

All CT morphological characteristics were evaluated in the lung window (level, –600 HU; width, 1,600 HU) by two experienced chest radiologists and two thoracic surgeons who were blinded to the pathological results of the nodules. The CT morphological characteristics, including median nodule diameter of the nodule (measured on the lung window), margin (coarse, smooth), vacuole (present, absent), lobulation (present, absent), spiculation (present, absent), pleural indentation (present, absent), and the location in the lung were evaluated with reference to the Fleischner Society's glossary of terms for thoracic imaging. All CT images were reviewed in random order.

Prediction model construction and validation

Univariate and multivariate analyses were conducted to select the independent predictors for distinguishing between pulmonary tuberculoma and lung cancer among non-calcified solid SPNs, and binary logistic regression analysis was performed to construct cooperated indicators. The backward elimination technique was used to define the best multivariate model, and the receiver operating characteristic (ROC) curve and the area under the curve (AUC) were applied to derive the diagnostic efficacy of the cooperated indicators in predicting pulmonary tuberculoma and lung cancer.

Statistical analysis

All statistical analyses were performed using SPSS software (version 24.0), and graphing was performed using GraphPad Prism 8.0. Categorical variables were expressed as frequencies and percentages and were analyzed with the Chi-square test or Fisher's exact test. Normally distributed continuous variables were expressed as the mean ± standard
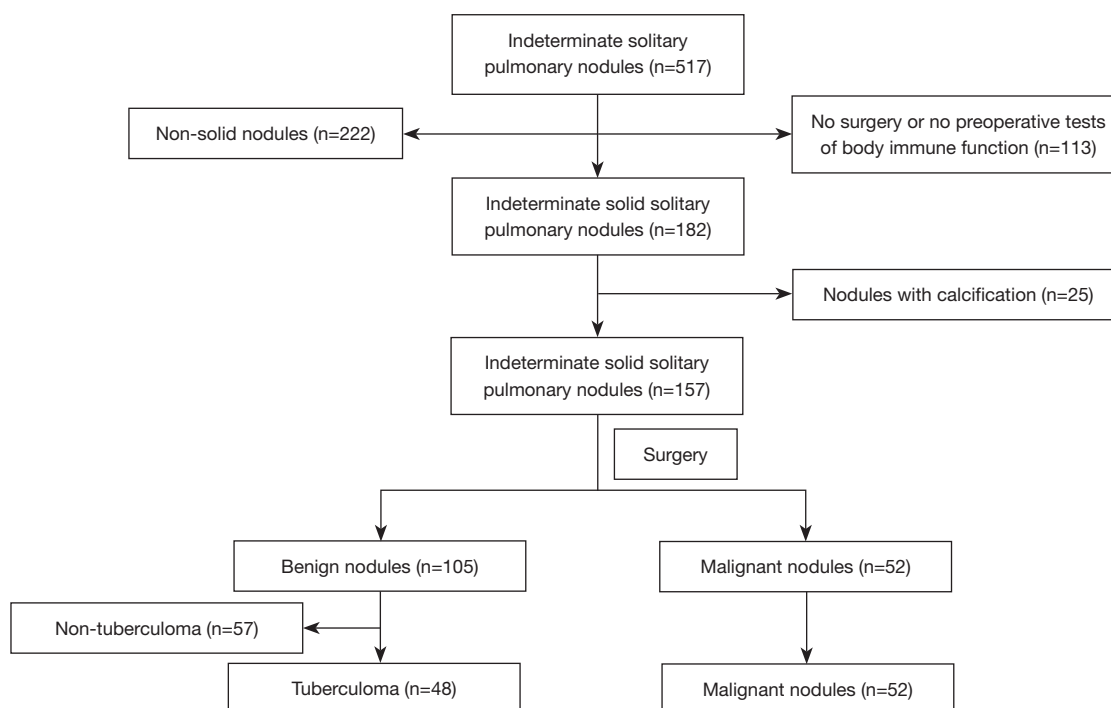
Figure 1 The flow chart for selecting patients.

deviation (SD) and were analyzed using an independent samples *t*-test. Non-normally distributed continuous variables were expressed as the median [Q1, Q3], and were analyzed with the Mann-Whitney test for two independent samples. Spearman's rank correlation test was employed to assess the correlations between the parameters, and strongly correlated parameters were excluded from further analysis.

The remaining significant variables in the univariate analysis were then included in a stepwise multivariate logistic regression analysis to select the optimal predictors for pulmonary tuberculoma. ROC curve analysis was conducted to derive the sensitivity, specificity, and accuracy of the selected variables in predicting pulmonary tuberculoma and lung cancer. P<0.05 was considered statistically significant.

Results

Clinical characteristics

We retrospectively reviewed a total of 517 patients with indeterminate solid SPNs. Of these patients, 113 patients were excluded as they had not undergone surgery or received preoperative immune function tests, 222

patients were excluded as they had non-solid nodules, and 25 patients were removed due to calcification. Of the remaining 157 patients, 105 were diagnosed with benign lesions and 52 with lung cancer. Among the 105 patients with benign lesions, 57 patients with non-tuberculoma were excluded. Finally, a total of 48 patients with non-calcified, solid, solitary pulmonary tuberculoma and 52 patients with solid lung cancer were included in this study. The patient selection process is simplified as a flow chart displayed in *Figure 1*.

The patients' clinical characteristics are shown in *Table 1*. There were no differences in the genders and ages of patients with pulmonary tuberculoma (31 males and 17 females; aged 56 years old, range: 46–63 years) and those with lung cancer (34 males and 18 females; aged 56 years old, range: 50–61 years). Only one patient in the pulmonary tuberculoma group was affected with pulmonary TB 20 years ago, and thus, there was no difference observed between the two groups. Moreover, there were 11 (22.92%) smokers with a history of heavy smoking in the pulmonary tuberculoma group and 14 (26.92%) smokers in the lung cancer group; however, this difference was not statistically significant. The clinical characteristics showed that the respective data of the two groups were comparable.

Table 1 Clinical characteristics between patients with pulmonary tuberculoma and those with malignancy

Characteristics	Total (N=100)	Tuberculoma (n=48)	Malignancy (n=52)	P value
Gender, n (%)				0.933[1]
Male	65 (65.00)	31 (64.58)	34 (65.38)	
Female	35 (35.00)	17 (35.42)	18 (34.62)	
Age (years)	56 [48–61]	56 [46–63]	56 [50–61]	0.600[2]
History of TB, n (%)				0.296[1]
Present	1 (1.00)	1 (2.08)	0 (0.00)	
Absent	99 (99.00)	47 (97.92)	52 (100.00)	
History of heavy smoking, n (%)				0.644[1]
Present	25 (25.00)	11 (22.92)	14 (26.92)	
Absent	75 (75.00)	37 (77.08)	38 (73.08)	

The data are expressed as n (%) or median [IQR]. [1], Pearson's chi-square test; [2], Mann-Whitney rank sum test. TB, tuberculosis; IQR, interquartile range.

CT imaging features

The CT semantic features of the pulmonary tuberculoma and lung cancer groups are shown in *Table 2*. There was no significant difference in the median nodule diameter between patients in the pulmonary tuberculoma (median 14 mm, range: 11–23 mm) and lung cancer (median 19 mm, range: 13–26 mm) groups (P>0.05). In terms of location, the data distribution of the two groups was roughly the same, and the difference was not statistically significant (P>0.05).

Univariate analysis showed that there were significant differences between the tuberculoma and lung cancer patients in terms of the vacuole, coarse margin, lobulation, spiculation, and pleural indentation (P<0.05, *Table 2*), which revealed that patients with tuberculoma had a significantly lower frequency of vacuole (12.50% *vs.* 38.45%, P=0.003), coarse margin (47.92% *vs.* 84.62%, P<0.001), lobulation (27.08% *vs.* 61.54%, P=0.001), spiculation (22.92% *vs.* 59.62%, P<0.001), and pleural indentation (16.17% *vs.* 53.85%, P<0.001) than those with lung cancer. *Figure 2* provides representative chest computed tomography images of noncalcified pulmonary tuberculoma and malignancy.

Immunocytes and tumor-related markers

Regarding immunocytes, the immunocyte levels in the peripheral blood of the tuberculoma group were higher than those in the lung cancer group (*Table 3*). Univariate analysis showed that there were marked differences between

patients with tuberculoma and lung cancer in terms of total lymphocyte count (P=0.050), CD3^{+} T-lymphocyte count (P=0.028), and CD4^{+} T-lymphocyte count (P=0.024); however, there were no significant differences in CD8^{+} T-lymphocyte count and the CD4^{+} T/CD8^{+} T. The data distribution characteristics for CD3^{+} T and CD4^{+} T lymphocyte counts are shown in *Figure 3*. As for tumor markers, there were no statistically significant differences between the two groups (P>0.05).

Prediction model construction and validation

Correlation analysis was performed on all continuous variables with P<0.05, which indicated that the CD3^{+} T-lymphocyte count was positively correlated with CD4^{+} T-lymphocyte count (r=0.845, P<0.001) and CD8^{+} T-lymphocyte count (r=0.834, P<0.001). Univariate and correlation analysis showed that a coarse margin, vacuole, lobulation, spiculation, pleural indentation, total lymphocyte count, CD3^{+} T-lymphocyte count, and CD4^{+} T-lymphocyte count were notably different between the two groups. Next, stepwise multivariate logistic regression analysis was performed to derive the optimal variables that could discriminate tuberculoma from lung cancer and to construct the predictive model.

Finally, a coarse margin, vacuole, lobulation, pleural indentation, CD3^{+} T lymphocyte count, and CD4^{+} T lymphocyte count were identified as independent risk factors aiding in differential diagnosis. Considering the

Table 2 Computed tomography imaging features between patients with pulmonary tuberculoma and those with malignancy

Characteristics	Total	Tuberculoma	Malignancy	P value
Nodule diameter (mm), median [IQR]	17 [11–24]	14 [11–23]	19 [13–26]	0.065[2]
Margin, n (%)				<0.001[1]
Smooth	33 (33.00)	25 (52.08)	8 (15.38)	
Coarse	67 (67.00)	23 (47.92)	44 (84.62)	
Vacuole, n (%)				0.003[1]
Present	26 (26.00)	6 (12.50)	20 (38.46)	
Absent	74 (74.00)	42 (87.50)	32 (61.54)	
Lobulation, n (%)				0.001[1]
Present	45 (45.00)	13 (27.08)	32 (61.54)	
Absent	55 (55.00)	35 (72.92)	20 (38.46)	
Spiculation, n (%)				<0.001[1]
Present	42 (42.00)	11 (22.92)	31 (59.62)	
Absent	58 (58.00)	37 (77.08)	21 (40.38)	
Pleural indentation, n (%)				<0.001[1]
Present	36 (36.00)	8 (16.67)	28 (53.85)	
Absent	64 (64.00)	40 (83.33)	24 (46.15)	
Location, n (%)				0.777[1]
RUL	32 (32.00)	15 (31.25)	17 (32.69)	
RML	7 (7.00)	3 (6.25)	4 (7.69)	
RLL	18 (18.00)	11 (22.92)	7 (13.46)	
LUL	22 (22.00)	9 (18.75)	13 (25.00)	
LLL	21 (21.00)	10 (20.83)	11 (21.15)	

[1], Pearson's chi-square test; [2], Mann-Whitney rank sum test. IQR, interquartile range; RUL, right upper lobe; RML, right middle lobe; RLL, right lower lobe; LUL, left upper lobe; LLL, left lower lobe.

correlation between the $CD3^+$ T-lymphocyte count and the $CD4^+$ T-lymphocyte count, they were respectively selected to construct the model with other variables and to obtain the ROC curves (model 1 included the $CD3^+$ T-lymphocyte count, and model 2 included the $CD4^+$ T-lymphocyte count). The AUC of model 1 was 0.845 [95% confidence interval (CI), 0.759–0.910], while model 2 had an AUC of 0.857 (95% CI, 0.773–0.919) (*Figure 4*). The sensitivity, specificity, and accuracy of model 1 in distinguishing pulmonary tuberculoma from lung cancer were 79.2%, 75%, and 74.5%, respectively, while those of model 2 were 77.1%, 78.8%, and 77.1%, respectively. Model 2 showed a superior ability to distinguish pulmonary tuberculoma from lung cancer among non-calcified solid SPNs. The Hosmer-Lemeshow test (P>0.05) and assessment of the bootstrap calibration curves suggested an adequate model fit.

Discussion

Benign nodules account for a large proportion of solid SPNs, the majority of which are pulmonary tuberculomas. Chemotherapy is the predominant treatment for pulmonary tuberculomas that are less than 3 cm (27), whereas solid lung cancers are mainly treated surgically, as the latter is considered to be highly malignant and invasive and has a poor prognosis (28,29). In our opinion, even though some literature (30) has indicated that surgery combined with postoperative anti-TB treatment is effective for
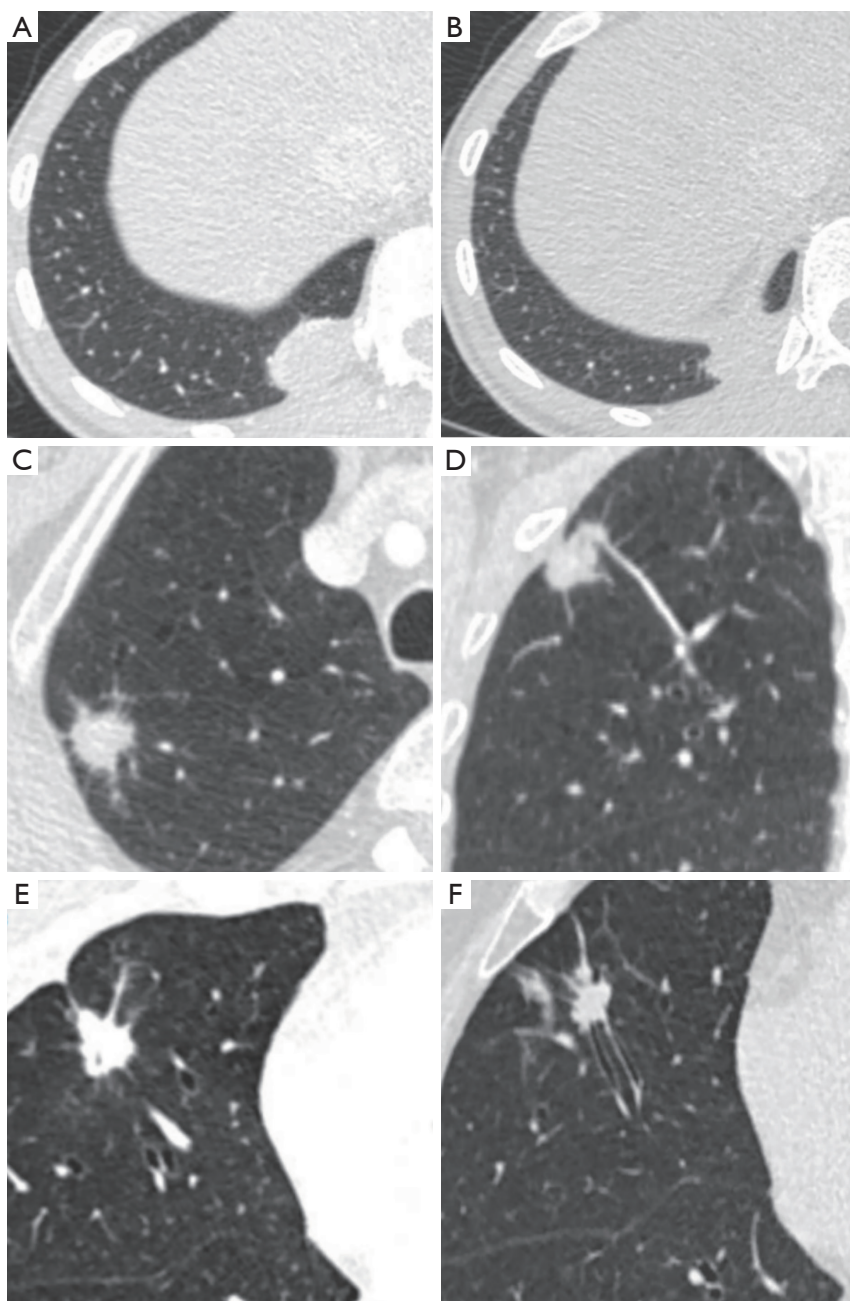
Figure 2 Representative chest computed tomography images of noncalcified pulmonary tuberculoma and malignancy. (A,B) A 30-year-old woman with typical pulmonary tuberculoma in the lower lobe of the right lung. Axial image (A) shows a round-like well-defined solid nodule with uniform density measuring 3.0 cm; (B) it connects to pleura and diaphragm by broad base without pleural indentation; the lesion was confirmed on pathological diagnosis as a tuberculoma. (C,D) A 65-year-old man with atypical pulmonary tuberculoma in the right lower lobe. Axial image (C) demonstrates a solid nodule measuring 1.4 cm with lobulation, long spiculation, and pleural indentation sign. Vascular convergence can be seen on the reconstructed coronal (D). His CD3+ T cell and CD4+ T cell count significantly increased, and the lesion was confirmed on pathological diagnosis as a tuberculoma. (E,F) A 69-year-old man with lung squamous cell carcinoma in the right middle lobe. Axial image (E) present as a well-defined solid nodule measuring 1.7 cm with lobulation, long spiculation, and pleural indentation sign. The next slice image (F) shows that intact and patent bronchi were obstructed abruptly by the SPN (F). The lesion was proved to be a squamous cell carcinoma on pathological diagnosis. SPN, solitary pulmonary nodule.

Table 3 Immunocyte counts and tumor-related markers between patients with pulmonary tuberculoma and those with malignancy

Characteristics	Total	Tuberculoma	Malignancy	P value
Total lymphocyte count (10^9/L)	1.83±0.59	1.95±0.72	1.71±0.42	0.050[3]
CD3$^+$ T lymphocyte count (10^9/L)	1.13 (0.92–1.50)	1.34 (0.92–1.69)	1.03 (0.92–1.32)	0.028[2]
CD4$^+$ T lymphocyte count (10^9/L)	0.63 (0.50–0.81)	0.72 (0.52–0.93)	0.58 (0.49–0.70)	0.024[2]
CD8$^+$ T lymphocyte count (10^9/L)	0.37 (0.30–0.51)	0.44 (0.28–0.57)	0.36 (0.31–0.46)	0.285[2]
CD4$^+$ T/CD8$^+$ T	1.67±0.55	1.74±0.60	1.60±0.49	0.208[3]
CYFRA21–1 (ng/mL), n (%)				0.787[1]
Normal (<3.3)	78 (78.00)	38 (79.17)	40 (76.92)	
Elevated (≥3.3)	22 (22.00)	10 (20.83)	12 (23.08)	
CEA (ng/mL), n (%)				0.823[1]
Normal (<5)	91 (91.00)	44 (91.67)	47 (90.38)	
Elevated (≥5)	9 (9.00)	4 (8.33)	5 (9.62)	

The data are expressed as n (%) or median (IQR) or mean ± SD. [1], Pearson's chi-square test; [2], Mann-Whitney rank sum test; [3], independent sample *t*-test. CYFRA21-1, cytokeratin fragment antigen 21-1; CEA, carcinoembryonic antigen; IQR, interquartile range; SD, standard deviation.

pulmonary tuberculoma, this does not mean that surgery combined with postoperative anti-TB treatment is the optimal therapeutic schedule. This may be because most tuberculomas are diagnosed by surgical biopsy, and there is currently a lack of effective non-surgical diagnostic tools. In this retrospective study, we evaluated the value of immune cell detection combined with CT imaging features for identifying pulmonary tuberculoma and lung cancer among non-calcified solid SPNs, aiming to find relatively objective indicators and establish effective predictive models.

The pathological findings of the 105 patients with benign lesions were as follows: 48 patients had tuberculoma, 37 patients had inflammatory pseudotumor, six patients had round pneumonia, four patients had organizing pneumonia, three patients had pulmonary sclerosing neurocytoma, three patients had hamartoma, three patients had a fungal infection, and one patient had a bronchogenic cyst. Tuberculoma remains a major part among these benign lesions. In terms of clinical characteristics, to make the data of patients with pulmonary tuberculoma and malignancy comparable, we enrolled two groups of patients with no differences in age and gender. Some previous studies (31,32) have shown that age and gender were independent risk factors for identifying patients with pulmonary tuberculoma and lung cancer, and most patients with tuberculoma were male and were often much younger than those with lung cancer. However, Choi *et al.* found that age and gender had

no diagnostic value by reviewing 107 cases of SPNs (33). In our study, there were no differences in other characteristics between the two groups, such as a history of TB and heavy smoking, which could be explained by the fact that a history of heavy smoking is a risk factor for both conditions. Also, patients with a history of pulmonary TB had a 1.23-fold increased risk of lung cancer (34,35).

CT morphological features are important for the early identification of benign and malignant solid pulmonary nodules and can serve as predictive factors for prognosis. In our study, the median nodule diameter (median, 14 mm) of atypical pulmonary tuberculomas was slightly smaller than that of lung cancers (median, 19mm), which is consistent with the conclusion of Liu *et al.* (36). Moreover, there were no significant differences between patients with pulmonary tuberculoma and lung cancer in terms of distribution, but both groups exhibited a significant upper lobe distribution advantage (50.00%, and 57.69%, respectively). This anatomic appearance may be attributed to hyperoxic tension and the relative lack of lymph drainage in the upper lobe region, which may promote the growth of Mycobacterium tuberculosis (37). The CT imaging signs, such as a vacuole, coarse margin, lobulation, spiculation, and pleural indentation, have been confirmed to be independent risk factors for identifying benign and malignant solid SPNs; however, there are few studies on the association with pulmonary tuberculoma. In our study, univariate
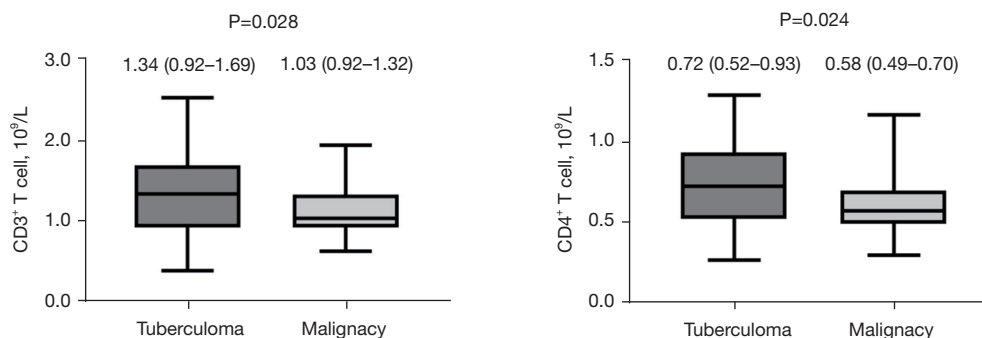
Figure 3 Boxplots showed the difference in data distribution of CD3+ T cell count and CD4+ T cell count between two groups.
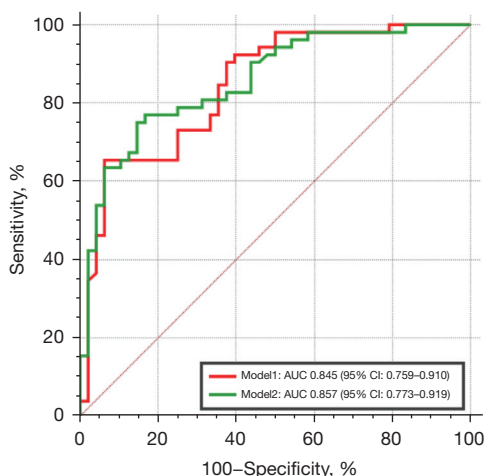
Figure 4 ROC curve applied to distinguish tuberculoma from malignancy; model 1 represents the model of CD3+ T cell count combined with CT morphological features; and model 2 represents the model of CD4+ T cell count combined with CT morphological features. ROC, receiver operating characteristic; CT, computed tomography.

analysis showed that there were statistical differences in the vacuoles, nodular margins, lobation, spiculation, and pleural indentation between pulmonary tuberculoma and malignancy, and patients with pulmonary tuberculoma had a significantly lower frequency of coarse margin, vacuole, lobulation, spiculation, and pleural indentation than those with lung cancer, which is consistent with the conclusions of previous studies (38,39).

In addition, there are also some relatively rare morphological features, such as satellite lesions, tree-in-bud pattern, air bronchogram, and vascular convergence, which also have a superior effect in distinguishing between pulmonary tuberculoma and malignancy. The tree-in-bud pattern, which was first described as a branching linear structure with more than one contiguous branching site by Im in 1993, is considered to be significantly associated with pulmonary tuberculoma, particularly active tuberculoma (40). Satellite lesions are typically described as small discrete shadows near the main lesion, and are associated with pulmonary tuberculoma (41). An air bronchogram is defined as a pattern of air-filled bronchi on a background of the airless lung, which can be divided into five types. Interestingly, the types in which bronchi are displaced, compressed, and narrowed by the SPN are more common in benign nodules, while those in which intact and patent bronchi are obstructed abruptly by the SPN were more common in malignant nodules. This phenomenon exists because of the lack of tumoral infiltration and the accompanying desmoplastic response (42). The vascular convergence sign refers to vessels converging to a nodule without adjoining or contacting the edge of the nodule. Angiogenesis is essential for tumor growth and metastasis and is primarily seen in peripheral lung cancers.

As important immune cells that mediate cellular immune responses, T cells can be divided into three categories, CD4+ helper T cells, CD8+ cytotoxic T cells, and regulatory T cells, which exert a variety of immunological effects. The level of T cells, which are also called CD3+ T cells, in the peripheral blood is related to the immune microenvironment of the body as well as the development of pulmonary tuberculoma and malignancy. In our study, the CD3+ and CD4+ T-cell counts were significantly higher in the peripheral blood of patients with pulmonary tuberculoma than in those with lung malignancy, suggesting that patients with pulmonary tuberculoma were in a relatively higher immune response state than those with lung cancer. Meanwhile, the lack of significant differences between the two groups in the serum levels of tumor-related markers confirmed the CD3+ and CD4+ T-cell counts as potential indicators for distinguishing

pulmonary tuberculoma from early malignancy.

Granuloma, which is considered to be the core lesion of tuberculoma, provides the immune environment required for the containment of bacteria. M.tuberculosis-specific T cells are crucial for granuloma maturation, maintenance, and control of the bacterial spread (43). CD4^{+} T cells are the dominant cells mediating the anti-TB response, which can serve as "innate-like" cells to prevent the dissemination of M.tuberculosis at the initial stage of TB infection, and as master helpers to maintain the multiple effector functions of CD8^{+} T cells and other lymphocytes during the development of adaptive immunity against primary TB (44). Saunders *et al.* exposed mice with a disruption to their CD4 gene to an aerosol of M.tuberculosis and found that the early growth of M.tuberculosis was independent of CD4^{+} T cells; however, these cells were required to facilitate the recruitment of mononuclear cells to the lung, thereby ensuring long-term survival (45). So, we speculated that the formation of pulmonary tuberculoma could be highly associated with CD4^{+} T cells.

TB/human immunodeficiency virus (HIV) co-infection is one of the greatest current public health challenges, and HIV infection increases the risk of active TB, leading to high mortality (46). The complex interaction between HIV and TB has not been elucidated. In our opinion, CD4^{+} T cells are the key to controlling the primary infection and conducting immunosurveillance of bacteria persisting in the granuloma, so that when CD4^{+} T cells in the lymphoid tissues and peripheral blood are depleted by HIV, the risk of progression from tuberculoma to active TB will significantly rise (47,48). In contrast, patients with lung malignancies prefer to be in a state of low immunity, because the tumor itself is not highly immunogenic, and the tumor microenvironment may inhibit the activity of tumor-specific T cells (49).

CD8^{+} T cells are considered to play a minor role in TB (50); however, our study showed that the levels of CD8^{+} T cells were not different between the two groups. This may be partly attributed to the limited sample size, and possibly, that CD8^{+} T cells might only have a minor contribution in the diagnosis of latent TB infection (51). However, the specific mechanism at play is not clear. Li *et al.* reported that pre-treated TB patients showed higher levels of CD8^{+} T cells in the peripheral blood than healthy controls and that CD8^{+} T-cell counts decreased during anti-TB therapy (52). As a result, we speculated that when TB transitions from the active to the stationary phase, like tuberculoma, the CD8^{+} T cells may return to normal.

Conclusions

Pulmonary tuberculoma and malignancy are two common kinds of intrapulmonary masses or nodular lesions in clinical practice, with significant differences between their treatments and clinical prognoses. Our study demonstrated that clinicians should be highly vigilant for pulmonary tuberculoma in cases of non-calcified solid SPNs without a coarse margin, vacuole, lobation, spiculation, and pleural indentation and combined with high CD3^{+} or CD4^{+} T-cell counts. We discovered that the immunocyte count can be used as a potential indicator for distinguishing pulmonary tuberculoma from early malignancy, which will be a starting point for our future research.

Our study has several limitations that should be considered. Firstly, to ensure that the data between the two groups of patients were comparable, our study had a relatively small sample size and a relatively large number of variables evaluated, which may also explain the low specificity of our prediction model. Secondly, we only focused on distinguishing between pulmonary tuberculoma and malignancy among non-calcified solid SPNs rather than other pathological types, and thus, our results should be interpreted carefully. Thirdly, our model is probably overfitting, since the ROC curves were constructed using the same data that the predictors were derived from.

For future research, a multicenter design with a large cohort and more indicators is needed to expand upon the present results. Also, the model presented in this study will be validated using an external dataset to evaluate its true predictive value.

Footnote

Reporting Checklist: The authors have completed the STROBE reporting checklist. Available at https://jtd.amegroups.com/article/view/10.21037/jtd-22-1024/rc

Data Sharing Statement: Available at https://jtd.amegroups.com/article/view/10.21037/jtd-22-1024/dss

References

1. Chakaya J, Khan M, Ntoumi F, et al. Global Tuberculosis Report 2020 - Reflections on the Global TB burden, treatment and prevention efforts. Int J Infect Dis 2021;113 Suppl 1:S7-S12.
2. Koenig SP, Furin J. Update in Tuberculosis/Pulmonary Infections 2015. Am J Respir Crit Care Med 2016;194:142-6.
3. Cardinale L, Parlatano D, Boccuzzi F, et al. The imaging spectrum of pulmonary tuberculosis. Acta Radiol 2015;56:557-64.
4. Harzheim D, Eberhardt R, Hoffmann H, et al. The Solitary Pulmonary Nodule. Respiration 2015;90:160-72.
5. Baldwin DR, Callister ME; . The British Thoracic Society guidelines on the investigation and management of pulmonary nodules. Thorax 2015;70:794-8.
6. Sun K, Chen S, Zhao J, et al. Convolutional Neural Network-Based Diagnostic Model for a Solid, Indeterminate Solitary Pulmonary Nodule or Mass on

7. She Y, Zhao L, Dai C, et al. Development and validation of a nomogram to estimate the pretest probability of cancer in Chinese patients with solid solitary pulmonary nodules: A multi-institutional study. J Surg Oncol 2017;116:756-62.
8. Andreu J, Cáceres J, Pallisa E, et al. Radiological manifestations of pulmonary tuberculosis. Eur J Radiol 2004;51:139-49.
9. Giller DB, Giller BD, Giller GV, et al. Treatment of pulmonary tuberculosis: past and present. Eur J Cardiothorac Surg 2018;53:967-72.
10. Zhang J, Han T, Ren J, et al. Discriminating Small-Sized (2 cm or Less), Noncalcified, Solitary Pulmonary Tuberculoma and Solid Lung Adenocarcinoma in Tuberculosis-Endemic Areas. Diagnostics (Basel) 2021.
11. Feng B, Chen X, Chen Y, et al. Radiomics nomogram for preoperative differentiation of lung tuberculoma from adenocarcinoma in solitary pulmonary solid nodule. Eur J Radiol 2020;128:109022.
12. Dullabh KJ, Maharaj K. Solitary pulmonary nodule and the surgeon. Afr J Thorac Crit Care Med 2020.
13. Albano D, Gatta R, Marini M, et al. Role of 18F-FDG PET/CT Radiomics Features in the Differential Diagnosis of Solitary Pulmonary Nodules: Diagnostic Accuracy and Comparison between Two Different PET/CT Scanners. J Clin Med 2021;10:5064.
14. Niyonkuru A, Chen X, Bakari KH, et al. Evaluation of the diagnostic efficacy of (18) F-Fluorine-2-Deoxy-D-Glucose PET/CT for lung cancer and pulmonary tuberculosis in a Tuberculosis-endemic Country. Cancer Med 2020;9:931-42.
15. Cysouw MCF, Golla SVS, Frings V, et al. Partial-volume correction in dynamic PET-CT: effect on tumor kinetic parameter estimation and validation of simplified metrics. EJNMMI Res 2019;9:12.
16. Mackin D, Ger R, Dodge C, et al. Effect of tube current on computed tomography radiomic features. Sci Rep 2018;8:2354.
17. Zhao J, Sun L, Sun K, et al. Development and Validation of a Radiomics Nomogram for Differentiating Pulmonary Cryptococcosis and Lung Adenocarcinoma in Solitary Pulmonary Solid Nodule. Front Oncol 2021;11:759840.
18. Fu L, Wang R, Yin L, et al. CYFRA21-1 tests in the diagnosis of non-small cell lung cancer: A meta-analysis. Int J Biol Markers 2019;34:251-61.
19. MOYES EN. Tuberculoma of the lung. Thorax 1951;6:238-49.
20. Co DO, Hogan LH, Karman J, et al. T Cell Interactions

in Mycobacterial Granulomas: Non-Specific T Cells Regulate Mycobacteria-Specific T Cells in Granulomatous Lesions. Cells 2021.

21. Gern BH, Adams KN, Plumlee CR, et al. TGFβ restricts expansion, survival, and function of T cells within the tuberculous granuloma. Cell Host Microbe 2021;29:594-606.e6.

22. Vallejo R, García Marín JF, Juste RA, et al. Immunohistochemical characterization of tuberculous lesions in sheep naturally infected with Mycobacterium bovis. BMC Vet Res 2018;14:154.

23. Ferluga J, Yasmin H, Al-Ahdal MN, et al. Natural and trained innate immunity against Mycobacterium tuberculosis. Immunobiology 2020;225:151951.

24. Shi J, Liu X, Ming Z, et al. Value of Combined Detection of Cytokines and Tumor Markers in the Differential Diagnosis of Benign and Malignant Solitary Pulmonary Nodules. Zhongguo Fei Ai Za Zhi 2021;24:426-33.

25. DeCotiis C, Hu Y, Greenberg AK, et al. Inflammatory cytokines and non-small cell lung cancer in a CT-scan screening cohort: Background review of the literature. Cancer Biomark 2016;16:219-33.

26. Ostroumov D, Fekete-Drimusz N, Saborowski M, et al. CD4 and CD8 T lymphocyte interplay in controlling tumor growth. Cell Mol Life Sci 2018;75:689-713.

27. Xia Z, Qiao K, He J. Recent advances in the management of pulmonary tuberculoma with focus on the use of tubeless video-assisted thoracoscopic surgery. J Thorac Dis 2017;9:3307-12.

28. Oda S, Awai K, Murao K, et al. Volume-doubling time of pulmonary nodules with ground glass opacity at multidetector CT: Assessment with computer-aided three-dimensional volumetry. Acad Radiol 2011;18:63-9.

29. Lee SM, Park CM, Paeng JC, et al. Accuracy and predictive features of FDG-PET/CT and CT for diagnosis of lymph node metastasis of T1 non-small-cell lung cancer manifesting as a subsolid nodule. Eur Radiol 2012;22:1556-63.

30. Subotic D, Yablonskiy P, Sulis G, et al. Surgery and pleuro-pulmonary tuberculosis: a scientific literature review. J Thorac Dis 2016;8:E474-85.

31. Lang S, Sun J, Wang X, et al. Asymptomatic pulmonary tuberculosis mimicking lung cancer on imaging: A retrospective study. Exp Ther Med 2017;14:2180-8.

32. Zhuo Y, Zhan Y, Zhang Z, et al. Clinical and CT Radiomics Nomogram for Preoperative Differentiation of Pulmonary Adenocarcinoma From Tuberculoma in Solitary Solid Nodule. Front Oncol 2021;11:701598.

33. Choi SM, Heo EY, Lee J, et al. Characteristics of benign solitary pulmonary nodules confirmed by diagnostic video-assisted thoracoscopic surgery. Clin Respir J 2016;10:181-8.

34. Zifodya JS, Crothers K. Tuberculosis, Chronic Obstructive Lung Disease, and Lung Cancer: The Holey Upper Lobe Trinity? Ann Am Thorac Soc 2022;19:540-2.

35. Novitskaya TA, Ariel BM, Dvorakovskaya IV, et al. Morphological characteristics of pulmonary tuberculosis concurrent with lung cancer. Arkh Patol 2021;83:19-24.

36. Liu Y, Balagurunathan Y, Atwater T, et al. Radiological Image Traits Predictive of Cancer Status in Pulmonary Nodules. Clin Cancer Res 2017;23:1442-9.

37. Buckner CB, Walker CW. Radiologic manifestations of adult tuberculosis. J Thorac Imaging 1990;5:28-37.

38. Snoeckx A, Reyntiens P, Desbuquoit D, et al. Evaluation of the solitary pulmonary nodule: size matters, but do not ignore the power of morphology. Insights Imaging 2018;9:73-86.

39. Wei S, Shi B, Zhang J, et al. Differentiating mass-like tuberculosis from lung cancer based on radiomics and CT features. Transl Cancer Res 2021;10:4454-63.

40. Im JG, Itoh H, Shim YS, et al. Pulmonary tuberculosis: CT findings--early active disease and sequential change with antituberculous therapy. Radiology 1993;186:653-60.

41. Wang XL, Shan W. Application of dynamic CT to identify lung cancer, pulmonary tuberculosis, and pulmonary inflammatory pseudotumor. Eur Rev Med Pharmacol Sci 2017;21:4804-9.

42. Qiang JW, Zhou KR, Lu G, et al. The relationship between solitary pulmonary nodules and bronchi: multi-slice CT-pathological correlation. Clin Radiol 2004;59:1121-7.

43. Carow B, Hauling T, Qian X, et al. Spatial and temporal localization of immune transcripts defines hallmarks and diversity in the tuberculosis granuloma. Nat Commun 2019;10:1823.

44. Yao S, Huang D, Chen CY, et al. CD4+ T cells contain early extrapulmonary tuberculosis (TB) dissemination and rapid TB progression and sustain multieffector functions of CD8+ T and CD3- lymphocytes: mechanisms of CD4+ T cell immunity. J Immunol 2014;192:2120-32.

45. Saunders BM, Frank AA, Orme IM, et al. CD4 is required for the development of a protective granulomatous response to pulmonary tuberculosis. Cell Immunol 2002;216:65-72.

46. Bell LCK, Noursadeghi M. Pathogenesis of HIV-1 and Mycobacterium tuberculosis co-infection. Nat Rev

Microbiol 2018;16:80-90.
47. Venturini E, Lodi L, Francolino I, et al. CD3, CD4, CD8, CD19 and CD16/CD56 positive cells in tuberculosis infection and disease: Peculiar features in children. Int J Immunopathol Pharmacol 2019;33:2058738419840241.
48. Sharan R, Bucşan AN, Ganatra S, et al. Chronic Immune Activation in TB/HIV Co-infection. Trends Microbiol 2020;28:619-32.
49. Borst J, Ahrends T, Bąbała N, et al. CD4(+) T cell help in cancer immunology and immunotherapy. Nat Rev Immunol 2018;18:635-47.
50. Lu YJ, Barreira-Silva P, Boyce S, et al. CD4 T cell help

prevents CD8 T cell exhaustion and promotes control of Mycobacterium tuberculosis infection. Cell Rep 2021;36:109696.
51. Tsuyuzaki M, Igari H, Okada N, et al. Role of CD8 T-cell in immune response to tuberculosis-specific antigen in QuantiFERON-TB Gold Plus. J Infect Chemother 2020;26:570-4.
52. Li G, Yang F, He X, et al. Anti-tuberculosis (TB) chemotherapy dynamically rescues Th1 and CD8+ T effector levels in Han Chinese pulmonary TB patients. Microbes Infect 2020;22:119-26.